6th International Conference on Advances in Experimental Structural Engineering
11th International Workshop on Advanced Smart Materials and Smart Structures Technology
August 1-2, 2015, University of Illinois, Urbana-Champaign, United States

Modal parameter identification of structures based on combining autocorrelation function and ERA under ambient excitation

Jianping HAN [1,2], Pengqiang AN [1,2]

1 Key Laboratory of Disaster Prevention and Mitigation in Civil Engineering of Gansu Province, Lanzhou University of Technology, Lanzhou, Gansu 730050, China
E-mail:jphan@lut.cn

2 Western Engineering Research Center of Disaster Mitigation in Civil Engineering of Ministry of Education, Lanzhou University of Technology, Lanzhou, Gansu 730050, China
E-mail:anpengqiang@163.com

ABSTRACT

It was derived that the autocorrelation function of the dynamic response at the gauge point under white noise excitation can be expressed as the superposition of a series of complex exponential functions and sine functions. This expression has the similar form with the impulse response function. In addition, the autocorrelation function and the impulse response function decay in the same way. Then, the approach for the modal parameter identification based on the autocorrelation functions obtained from time domain response data under ambient excitation and the eigensystem realization algorithm (ERA) was proposed. Furthermore, the proposed identification approach was programmed via MATLAB. Finally, based on the ambient vibration test data, modal frequencies, damping ratios and mode shapes of a rigid frame-continuous girders bridge were identified by the proposed approach. Comparison with the identification results by a commercial modal analysis software indicates that the proposed approach is feasible and valid for identifying the modal parameters of the structure under ambient vibration.

KEYWORDS: *modal parameter identification, autocorrelation function, eigensystem realization algorithm, ambient vibration, rigid frame-continuous girders bridge*

1. INTRODUCTION

The structural test based on ambient vibration does not need extra excitation equipment and has no damage to the structure. And the structural modal parameters can be identified by only the response data. It is very significant to identify modal parameter of structures under ambient excitation for the condition assessment, damage detection and fault diagnosis. Therefore, the methods to identify modal parameters of the structure with the data of ambient vibration had been given increasing attention [1-7].

In recent years, the method combining Natural Excitation Technique (NExT) [8] with Eigensystem Realization Algorithm (ERA) [9] to identify modal parameters has become mature. The basic idea of this method is to take the cross-correlation function which is evaluated from the response data between two gauge points of the structure as the input of ERA to identify modal parameters.

In this paper, the approach combining autocorrelation function with ERA to identify modal parameters was proposed. Firstly, the expression of autocorrelation function of the dynamic response at the gauge point, which is superposed by a series of complex exponential functions and sine functions, was derived. This expression has the similar form with the impulse response function of the structure. In addition, the autocorrelation function and the impulse response function decay in the same way. Furthermore, the approach for identifying modal parameters based on the autocorrelation functions obtained from time domain response data under ambient excitation and ERA was proposed. And the proposed identification algorithm is programmed via MATLAB. Finally, based on the ambient vibration test data of a rigid frame-continuous girders bridge, modal frequencies, modal damping ratios and mode shapes of this bridge were identified by the proposed approach. In order to verfiy the feasibility and validity of the proposed approach, the identification results were compared with the results from a commercial modal analysis software .

2. THEORETICAL DERIVATION OF AUTOCORRELATION FUNCTION AS AN INPUT FOR ERA

The autocorrelation function of a random process describes the correlation between the values in a record at different instants of time. It is defined as the expected value of the product of a random variable $x(t)$ with a time-shifted version of itself [10].

The equations of motion of the Multiple-Degree-of-Freedom (MDOF) system in the modal coordinates result in [9],

$$\ddot{q}^r(t)+2\xi^r\omega_n^r\dot{q}^r(t)+\omega_n^{r2}q^r(t)=\frac{1}{m^r}\boldsymbol{\phi}^{r^T}\boldsymbol{f}(t) \tag{2.1}$$

where, $q^r(t)$ is the rth modal coordinate, ξ^r is the rth modal damping ratio, ω_n^r is the rth modal natural frequency, m^r is the rth modal mass, $\boldsymbol{\phi}^r$ is the rth mode shape vector, $\boldsymbol{f}(t)$ is a random excitation vector.

Due to a single input force $f_k(t)$ at the point k, the response $x_{ik}(t)$ at the point i is

$$x_{ik}(t)=\sum_{r=1}^{n}\phi_i^r\phi_k^r\cdot\int_{-\infty}^{t}f_k(\tau)g^r(t-\tau)d\tau \tag{2.2}$$

where n is the number of vibration modes, ϕ_i^r is the ith component of the rth mode shape vector, $g^r(t)=\frac{1}{m^r\omega_d^r}\exp\left(-\xi^r\omega_n^r t\right)\sin\left(\omega_d^r t\right)$ and $\omega_d^r=\omega_n^r\sqrt{1-(\xi^r)^2}$ is the rth damped modal natural frequency.

When the system is excited by an unit impulse $\delta(t)$ at the point k with $\delta(t)=\begin{cases}0 & (t\neq 0)\\ \infty & (t=0)\end{cases}$ and $\int_{-\infty}^{\infty}\delta(t)dt=1$, the system impulse response $h_{ik}(t)$ at the point i can be obtained from Eq. 2.2,

$$h_{ik}(t)=\sum_{r=1}^{n}\frac{\phi_i^r\phi_k^r}{m^r\omega_d^r}\exp(-\xi^r\omega_n^r t)\sin(\omega_d^r t) \tag{2.3}$$

Inputing white noise excitation at the point *k*, the autocorrelation function of the output $x(t)$ at the point i is defined as the following [11],

$$R_{iik}(\tau)=E\left[x_{ik}(t+\tau)x_{ik}(t)\right] \tag{2.4}$$

Substituting Eq. 2.2 into Eq. 2.4, $R_{iik}(\tau)$ can be rewritten as

$$\begin{aligned}R_{iik}(\tau)&=E\left\{\left[\sum_{r=1}^{n}\phi_i^r\phi_k^r\cdot\int_{-\infty}^{t+\tau}f_k(\sigma)g^r(t+\tau-\sigma)d\sigma\right]\cdot\left[\sum_{s=1}^{n}\phi_i^s\phi_k^s\cdot\int_{-\infty}^{t}f_k(\tau)g^s(t-\tau)d\tau\right]\right\}\\&=\sum_{r=1}^{n}\sum_{s=1}^{n}\phi_i^r\phi_k^r\phi_i^s\phi_k^s\cdot\int_{-\infty}^{t}\int_{-\infty}^{t+\tau}g^r(t+\tau-\sigma)g^s(t-\tau)E\left[f_k(\sigma)f_k(\tau)\right]d\sigma d\tau\end{aligned} \tag{2.5}$$

It is assumed that $f(t)$ is the ideal white noise and according to the definition of the correlation function in literature [11], we have

$$E\left[f_k(\tau)f_k(\sigma)\right]=a_k\sigma(\tau-\sigma) \tag{2.6}$$

where $\delta(t)$ is impulse response function; a_k is the constant term only related to the excitation at the point k.

Substituting Eq. 2.6 into Eq. 2.5 and integrating, we have

$$\begin{aligned} R_{iik}(\tau) &= \sum_{r=1}^{n}\sum_{s=1}^{n}\phi_i^r\phi_k^r\phi_i^s\phi_k^s\cdot\int_{-\infty}^{t}\int_{-\infty}^{t+\tau}g^r(t+\tau-\sigma)g^s(t-\tau)\cdot a_k\delta(\tau-\sigma)\,d\sigma\,d\tau \\ &= \sum_{r=1}^{n}\sum_{s=1}^{n}a_k\phi_i^r\phi_k^r\phi_i^s\phi_k^s\cdot\int_{-\infty}^{t}g^r(t+\tau-\tau)g^s(t-\tau)\,d\tau \end{aligned} \tag{2.7}$$

Taking $\lambda = T-\tau$, we have

$$R_{iik}(T) = \sum_{r=1}^{n}\sum_{s=1}^{n}a_k\phi_i^r\phi_k^r\phi_i^s\phi_k^s\cdot\int_{0}^{\infty}g^r(\lambda+T)g^s(\lambda)\,d\tau \tag{2.8}$$

Separating T and λ from $g^r(\lambda+T)$ by trigonometric function, we have

$$\begin{aligned} g^r(\lambda+T) &= \frac{1}{m^r\omega_d^r}\exp\left(-\xi^r\omega_n^r(\lambda+T)\right)\cdot\sin\left(\omega_d^r(\lambda+T)\right) \\ &= \left[\exp\left(-\xi^r\omega_n^rT\right)\cos(\omega_d^rT)\right]\frac{\exp\left(-\xi^r\omega_n^r\lambda\right)\sin\left(\omega_d^r\lambda\right)}{m^r\omega_d^r} \\ &+\left[\exp\left(-\xi^r\omega_n^rT\right)\sin(\omega_d^rT)\right]\frac{\exp\left(-\xi^r\omega_n^r\lambda\right)\cos\left(\omega_d^r\lambda\right)}{m^r\omega_d^r} \end{aligned} \tag{2.9}$$

Substituting Eq. 2.9 into Eq. 2.8, we have

$$\begin{aligned} &R_{iik}(T) = \sum_{r=1}^{n}\sum_{s=1}^{n}a_k\phi_i^r\phi_k^r\phi_i^s\phi_k^s\cdot \\ &\int_0^{\infty}\left(\begin{Bmatrix}\left[\exp\left(-\xi^r\omega_n^rT\right)\cos\left(\omega_d^rT\right)\right]\dfrac{\exp\left(-\xi^r\omega_n^r\lambda\right)\sin\left(\omega_d^r\lambda\right)}{m^r\omega_d^r}+\\ \left[\exp\left(-\xi^r\omega_n^rT\right)\sin\left(\omega_d^rT\right)\right]\dfrac{\exp\left(-\xi^r\omega_n^r\lambda\right)\cos\left(\omega_d^r\lambda\right)}{m^r\omega_d^r}\end{Bmatrix}\cdot\left\{\frac{\exp\left(-\xi^s\omega_n^s\lambda\right)\sin\left(\omega_d^s\lambda\right)}{m^s\omega_d^s}\right\}\right)d\lambda \\ &= \sum_{r=1}^{n}\begin{Bmatrix}\sum_{s=1}^{n}\dfrac{a_k\phi_i^r\phi_k^r\phi_i^s\phi_k^s}{m^r\omega_d^rm^s\omega_d^s}\left[\int_0^{\infty}\left[\exp\left[\left(-\xi^r\omega_n^r-\xi^s\omega_n^s\right)\cdot\lambda\right]\cdot\sin\left(\omega_d^s\lambda\right)\sin\left(\omega_d^r\lambda\right)\right]d\lambda\right]\cdot\exp\left(-\xi^r\omega_n^rT\right)\cos\left(\omega_d^rT\right)+\\ \sum_{s=1}^{n}\dfrac{a_k\phi_i^r\phi_k^r\phi_i^s\phi_k^s}{m^r\omega_d^rm^s\omega_d^s}\left[\int_0^{\infty}\left[\exp\left[\left(-\xi^r\omega_n^r-\xi^s\omega_n^s\right)\cdot\lambda\right]\cdot\sin\left(\omega_d^s\lambda\right)\cos\left(\omega_d^r\lambda\right)\right]d\lambda\right]\cdot\exp\left(-\xi^r\omega_n^rT\right)\sin\left(\omega_d^rT\right)\end{Bmatrix} \\ &= \sum_{r=1}^{n}\frac{\phi_i^r\phi_k^r}{m^r\omega_d^r}\exp\left(-\xi^r\omega_n^rT\right)\begin{Bmatrix}\sum_{s=1}^{n}\dfrac{a_k\phi_i^s\phi_k^s}{m^s\omega_d^s}\left[\int_0^{\infty}\left[\exp\left[\left(-\xi^r\omega_n^r-\xi^s\omega_n^s\right)\cdot\lambda\right]\sin\left(\omega_d^s\lambda\right)\sin\left(\omega_d^r\lambda\right)\right]d\lambda\right]\cdot\cos\left(\omega_d^rT\right)+\\ \sum_{s=1}^{n}\dfrac{a_k\phi_i^s\phi_k^s}{m^s\omega_d^s}\left[\int_0^{\infty}\left[\exp\left[\left(-\xi^r\omega_n^r-\xi^s\omega_n^s\right)\cdot\lambda\right]\sin\left(\omega_d^s\lambda\right)\cos\left(\omega_d^r\lambda\right)\right]d\lambda\right]\cdot\sin\left(\omega_d^rT\right)\end{Bmatrix} \end{aligned} \tag{2.10}$$

In Eq. 2.10, take

$$A = \sum_{s=1}^{n}\frac{a_k\phi_i^s\phi_k^s}{m^s\omega_d^s}\left[\int_0^{\infty}\left[\exp\left[\left(-\xi^r\omega_n^r-\xi^s\omega_n^s\right)\cdot\lambda\right]\cdot\sin\left(\omega_d^s\lambda\right)\sin\left(\omega_d^r\lambda\right)\right]d\lambda\right]$$

$$B = \sum_{s=1}^{n}\frac{a_k\phi_i^s\phi_k^s}{m^s\omega_d^s}\left[\int_0^{\infty}\left[\exp\left[\left(-\xi^r\omega_n^r-\xi^s\omega_n^s\right)\cdot\lambda\right]\cdot\sin\left(\omega_d^s\lambda\right)\cos\left(\omega_d^r\lambda\right)\right]d\lambda\right]$$

Eq. 2.10 becomes

$$\begin{aligned} R_{iik}(T) &= \sum_{r=1}^{n} \frac{\phi_i^r \phi_k^r}{m^r \omega_d^r} \exp\left(-\xi^r \omega_n^r T\right)\left[A\cos\left(\omega_d^r T\right) + B\sin\left(\omega_d^r T\right)\right] \\ &= \sum_{r=1}^{n} \frac{\phi_i^r \phi_k^r}{m^r \omega_d^r} \exp\left(-\xi^r \omega_n^r T\right)\left[\sqrt{A^2+B^2}\sin\left(\omega_d^r T + \theta\right)\right] \end{aligned} \tag{2.11}$$

where $\theta = \arcsin\left(\frac{A}{\sqrt{A^2+B^2}}\right)$.

Furthermore, Eq. 2.11 can be simplified as

$$R_{iik}(T) = \sum_{r=1}^{n} \frac{\phi_i^r C_i^r}{m^r \omega_d^r} \exp\left(-\xi^r \omega_n^r T\right)\sin\left(\omega_d^r T + \theta\right) \tag{2.12}$$

where C_i^r is the constant term only related to the mode order.

Comparing Eq. 2.3 with Eq. 2.12, it shows that both the expression of autocorrelation function and impulse response function at the any point are superposed by a series of complex exponential function and sine function. The autocorrelation function and the impulse response function decay in the same way. Therefore, the impulse response function can be replaced by autocorrelation function as input of ERA to identify modal parameters.

3. EIGENSYSTEM REALIZATION ALGORITHM

ERA is a time-domain modal parameter identification method in which the system order and system matrix $\boldsymbol{A}$, input matrix $\boldsymbol{B}$, output matrix $\boldsymbol{C}$ are determined by constructing generalized Hankel matrix and using singular value decomposition method. The modal parameters of the system can be obtained by the eigenvalues of the system matrix $\boldsymbol{A}$. More details on algorithm formula can be found in the literature [8]. Combining modal stabilization diagram with modal assurance criterion (MAC), false modes are eliminated in this paper.

Autocorrelation function matrix of all gauge points at each discrete time is

$$\boldsymbol{R}(k) = \left[R_{11}(k)\text{L}\ R_{ii}(k)\text{L}\ R_{NN}(k)\right]^T \tag{3.1}$$

where $R_{ii}(k)$ represents autocorrelation function values of the gauge point i at the discrete time k, N represents the amount of total gauge points.

Hankel matrix is structured by using autocorrelation function matrix $\boldsymbol{R}(k)$, we have

$$\boldsymbol{H}(k) = \begin{bmatrix} \boldsymbol{R}(k) & \boldsymbol{R}(k+1) & \text{L} & \boldsymbol{R}(k+s) \\ \boldsymbol{R}(k+1) & \boldsymbol{R}(k+2) & \text{L} & \boldsymbol{R}(k+s+1) \\ \boldsymbol{R}(k+2) & \text{M} & & \text{M} \\ \text{M} & \text{M} & & \text{M} \\ \boldsymbol{R}(k+r) & \boldsymbol{R}(r+k+1) & \text{L} & \boldsymbol{R}(k+r+s) \end{bmatrix} \tag{3.2}$$

And then matrix $\boldsymbol{H}(0)$, while $k=0$ in Hankel matrix, is constructed to evaluate modal parameters of the system. More details can be found in the literature [6, 8].

For that the test has multiple groups, the entire mode shape is formed by the reference point. Now, we take odd gauge points as an example to illustrate the step of modal assembling. For the case study of this paper, location of gauge points is shown in Fig. 4.2 and the testing program is shown in Table 4.1. First, mode shape coefficient of gauge points in each group is normalized by the way of making that mode shape coefficient of reference point is 1. And we have,

$$\left\{\begin{array}{c}1\\ \phi_1\\ \phi_3\\ \phi_5\end{array}\right\},\ \mathrm{K}\ ,\left\{\begin{array}{c}1\\ \phi_{19}\\ \phi_{21}\\ \phi_{23}\end{array}\right\},\ \mathrm{K}\ ,\left\{\begin{array}{c}1\\ \phi_{37}\\ \phi_{39}\\ \phi_{41}\end{array}\right\} \tag{3.3}$$

where ϕ_i is the mode shape coefficient of the gauge point i.

And then the overall mode shape is formulated with the help of mode shape coefficient 1 of the reference point and the location of gauge points,

$$\{\phi_1,\ \phi_3,\ \mathrm{L}\ ,\ \phi_{19},\ \phi_{21},\ \phi_{23},\ \mathrm{L}\ ,\ \phi_{39},\ \phi_{41}\}^T \tag{3.4}$$

Finally, the overall mode shape is normalized by making the mode shape coefficient, whose absolute value is maximum, is 1. Suppose the maximum mode shape coefficient is located in gauge point k, ϕ_k=1, and mode shape coefficient is normalized with ϕ_k=1. The final overall mode shape is:

$$\frac{1}{\phi_k}\cdot\{\phi_1,\ \phi_3,\ \mathrm{L}\ ,\ \phi_{19},\ \phi_{21},\ \phi_{23},\ \mathrm{L}\ ,\ \phi_{39},\ \phi_{41}\}^T \tag{3.5}$$

4. AMBIENT VIBRATION TESTING OF A RIGID FRAME-CONTINUOUS GIRDERS BRIDGE

The tested structure is a rigid frame-continuous girders bridge, which is shown in Fig. 4.1. The data of velocity were recorded by DH5907 date collection software with 50Hz sampling frequency and 900s sampling time. With wireless sensors, the data in both transverse and vertical directions can be collected. The location of velocity sensors is shown in Fig. 4.2, and the testing program is shown in Table 4.1. There are 42 gauge points in all which are divided into 7 testing sets, each of which contains 6 movable gauge points and a fixed reference point C20. The velocity time history records of the gauge point C1 and point C20 are shown in Fig. 4.3.

Figure 4.1 The main structure of the tested bridge

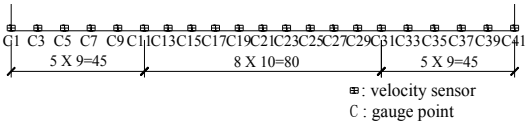

Figure 4.2 Location of gauge points

Table 4.1 Testing program

CH / GR	1	2	3	4	5	6	7
Group1	C20	C1	C2	C3	C4	C5	C6
Group2	C20	C7	C8	C9	C10	C11	C12
Group3	C20	C13	C14	C15	C16	C17	C18
Group4	C20	C19	C20	C21	C22	C23	C24
Group5	C20	C25	C26	C27	C28	C29	C30
Group6	C20	C31	C32	C33	C34	C35	C36
Group7	C20	C37	C38	C39	C40	C41	C42

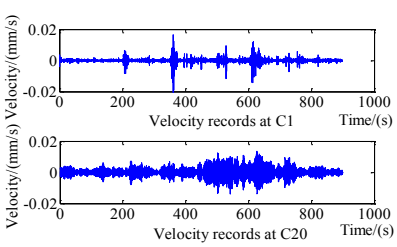

Figure 4.3 Vertical velocity time history records at the gauge points C1 and C20

5. IDENTIFICATION OF MODAL PARAMETER OF THE TESTED BRIDGE

Based on the transverse and vertical data of the tested bridge under ambient excitation, the transverse and vertical modal parameters of the bridge was identified by the proposed approach in this paper with MATLAB programme and DH5907, a commercial modal analysis software.

5.1. Identification results of the transverse modes

Table 5.1 is the comparison of the identification results of the transverse modal frequency and modal damping ratio between the proposed approach in this paper and DH5907. The evaluated autocorrelation function of the gauge point C11 is shown in Fig. 5.1. Fig. 5.2 is the stability diagram of the system, in which the system order changes from 2 to 35. The first three transverse modal frequencies of the system can be clearly seen in the Fig. 5.2.

Table 5.1 Identified transverse modal parameters

Modal order		Proposed algorithm			DH5907	
		Frequency /Hz	Damping ratio / %	MAC	Frequency /Hz	Damping ratio /%
Transverse	1	1.167	0.834	0.998	1.17	1.84
	2	2.601	0.750	0.991	2.61	1.17
	3	5.095	0.621	0.981	5.11	0.68

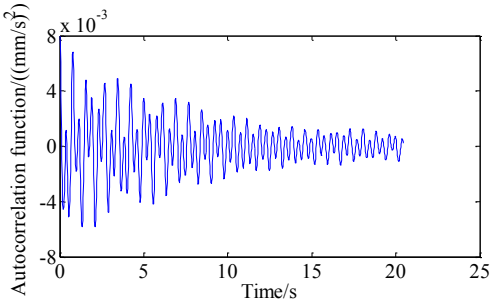

Figure 5.1 Autocorrelation function of transverse velocity at the gauge point C11

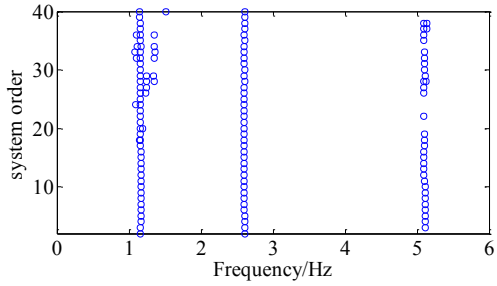

Figure 5.2 Stability diagram for transverse modes

Fig. 5.3 shows the first three transverse mode shapes identified by proposed approach in this paper. And Fig. 5.4 shows the first three transverse mode shapes identified by the modal analysis software DH5907.

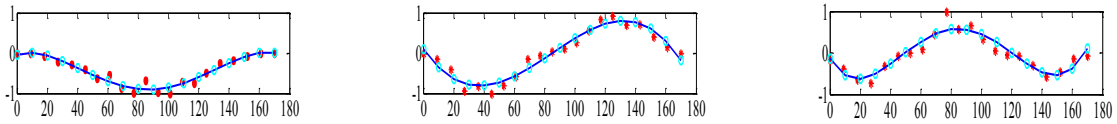

The 1st transverse mode shape The 2nd transverse mode shape The 3rd transverse mode shape

Figure 5.3 The first three transverse mode shapes identified by the proposed approach

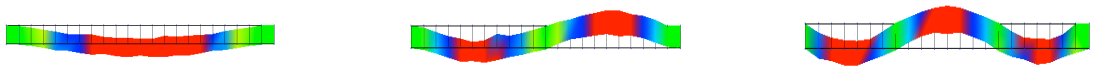

The 1st transverse mode shape The 2nd transverse mode shape The 3rd transverse mode shape

Figure 5.4 The first three transverse mode shapes identified by DH5907

5.2. Identification results of the vertical modes

Table 5.2 is the comparison of the identification results of the vertical modal frequency and damping ratio between the proposed approach in this paper and DH5907. The evaluated autocorrelation function of the gauge point C5 is shown in Fig. 5.5. Fig. 5.6 is the stability diagram of the system, in which the system order changes

from 2 to 35. The first four vertical mode frequencies of the system can be clearly seen in the Fig. 5.6.

Table 5.2 Identified vertical modal parameters

Modal order		Proposed algorithm		MAC	DH5907	
		Frequency /Hz	Damping ratio / %		Frequency /Hz	Damping ratio /%
Vertical	1	1.825	0.495	0.998	1.83	1.35
	2	2.877	0.770	0.991	2.88	1.04
	3	3.825	0.710	0.996	3.81	1.28
	4	4.694	0.625	0.993	4.69	0.73

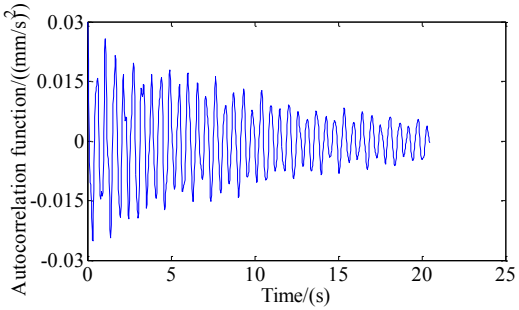

Figure 5. .5 Autocorrelation function of vertical velocity at the gauge point C5

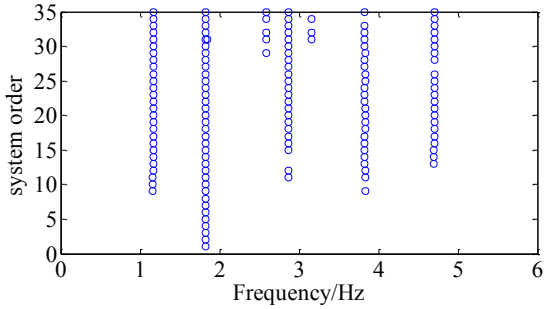

Figure 5.6 Stability diagram for vertical modes

Fig. 5.7 shows the first four vertical mode shapes identified by the proposed approach in this paper. And Fig. 5.8 shows the first four vertical transverse mode shapes identified by the modal analysis software DH5907.

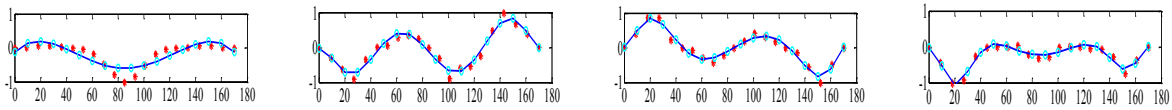

The 1st vertical mode shape | The 2nd vertical mode shape | The 3rd vertical mode shape | The 4th vertical mode shape

Figure 5.7 The first four vertical mode shapes identified by the proposed approach

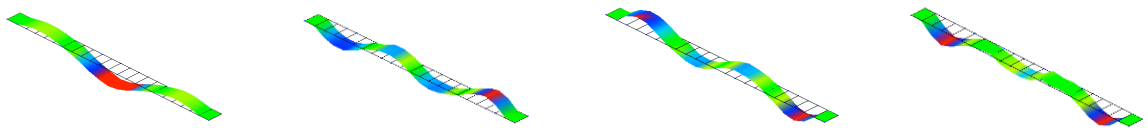

The 1st vertical mode shape | The 2nd vertical mode shape | The 3rd vertical mode shape | The 4th vertical mode shape

Figure 5.8 The first four vertical mode shapes identified by DH5907

5.3. Discussion of the modal parameter identification results

The comparison of the modal parameter identification results from the proposed approach in this paper and the commercial software has shown a basic consistency in the identification results of the modal frequencies and mode shapes, both for transverse and vertical direction. But there still is a big difference in the identification results of the modal damping ratios, as mentioned in the previous research findings [6, 12].

6. CONCLUSION

In this paper, under white noise excitation, the expression of autocorrelation function of the dynamic response at the gauge point, which is superposed by a series of complex exponential function and sine function, was derived. This expression has the similar form with the impulse response function. In addition, the autocorrelation function and the impulse response function decay in the same way. Based on the above theory, the approach for the modal parameter identification based on the autocorrelation functions obtained from time domain response data under ambient excitation and the eigensystem realization algorithm (ERA) was proposed. Furthermore, the proposed identification approach was programmed via MATLAB. Finally, based on the ambient vibration test data, modal frequencies, damping ratios and mode shapes of a rigid frame-continuous girders bridge were identified by the proposed approach. Comparison with the identification results by a commercial modal analysis software indicates that the proposed approach is feasible and valid for identifying the modal parameters of the structure under ambient vibration.

Therefore, combining autocorrelation function with the ERA algorithm can effectively identify the modal parameters of the structure under ambient excitation, which provides an alternative way to identify modal parameters of the structure under ambient excitation.

REFENCES

1. Doebling, S. W., Farrar, C. R., Prime, M. B., and Shevitz, D.W. (1996). *Damage Identification and Health Monitoring of Structural and Mechanical Systems from Changes in Their Vibration Characteristics. A Literature Review*. Los Alamos National Laboratory, Los Alamos, New Mexico.
2. Sohn, H., Farrar, C. R., Hemez, F. M., Shunk, D. D., Stinemates, D. W., Nadler, B. R., and Czarnecki, J. J. (2004). *A Review of Structural Health Monitoring Literature: 1996–2001*. Los Alamos National Laboratory, Los Alamos, New Mexico.
3. Brownjohn, J. M. W. (2004). Structural Health Monitoring of Civil Infrastructure. *Philosophical Transactions of the Royal Society A: Mathematical, Physical and Engineering Sciences*. **365:1851**, 589-622.
4. Brownjohn, J. M. W., Moyo, P., Omenzetter, P., and Lu, Y. (2003). Assessment of Highway Bridge Upgrading by Dynamic Testing and Finite Element Model Updating. *Journal of Bridge Engineering*. **8:3**, 162-172.
5. Maeck, J., Peeters, B., De Roeck, G. (2001). Damage Identification on the Z24 Bridge Using Vibration Monitoring. *Smart Material and Structures*. **10:3**, 512-517.
6. Han, J., Zheng, P., Luo, Y., Xie, Q., and Wang, C. (2013). Modal Parameter Identification of a Rigid Frame-Continuous Girders Bridge under Ambient Excitation. *Engineering Mechanics*. **30:S1**, 99-103.
7. Zhang, Y., Sim, S. H., Spencer, B. F., and Xiao, J. (2011). Reference Channel Selection Strategy in System Identification of Bridge Structure. *Journal of Vibration and Shock*. **30:12**, 181-184.
8. James, G. H., Carne, T. G., and Lauffer, J. P. (1995). The Natural Excitation Technique for Modal Parameter Extraction from Operating Structures. *Modal Analysis - The International Journal of Analytical and Experimental Modal Analysis*.**10:4**, 260-277.
9. Juang, J. N., and Pappa, R. S. (1985). An Eigensystem Realization Algorithm (ERA) for Modal Parameter Identification and Model Reduction. *Journal of Guidance Control and Dynamics*. **8:5**, 620-627.
10. Wang, J., and Hu, X. (2006). The Application of MATLAB in Vibration Signal Processing, China Water Conservancy and Hydropower Press, Beijing.
11. Papoulis, A. (1965). Probability, Random Variables, and Stochastic Processes, McGraw-Hill, New York.
12. Han, J., and Li, D. (2010). Modal Parameter Identification Based on Hilbert-Huang Transform and Natural Excitation Technique. *Engineering Mechanics*, **27:8**, 54-59.